DOI: 10.1021/cg900788h

CRYSTAL GROWTH & DESIGN Article

2009, Vol. 9
5273–5282

Co(II) Metal−Organic Frameworks (MOFs) Assembled from Asymmetric Semirigid Multicarboxylate Ligands: Synthesis, Crystal Structures, and Magnetic Properties

Hailong Wang, Daopeng Zhang, Daofeng Sun, Yuting Chen, Li-Fang Zhang, Laijin Tian, Jianzhuang Jiang,* and Zhong-Hai Ni*

Department of Chemistry, Shandong University, Jinan 250100, China

Received July 10, 2009; Revised Manuscript Received August 24, 2009

ABSTRACT: A series of four new coordination polymers, namely, $[Co(HL^1)(\mu\text{-}4,4'\text{-bpy})(H_2O)_3]_n\cdot(4,4'\text{-bpy})_n\cdot(H_2O)_{2n}$ (**1**), $[Co_{1.5}(L^2)(\mu\text{-}4,4'\text{-bpy})_{1.5}]_n\cdot(4,4'\text{-bpy})_{0.5n}$ (**2**), $[Co_3(L^3)(HL^3)(OH)(H_2O)_2(\mu\text{-}4,4'\text{-bpy})_2]_n\cdot(H_2O)_{2.5n}$ (**3**), and $[Co_{1.5}(L^4)(\mu\text{-}4,4'\text{-bpy})_2(H_2O)_3]_n\cdot(H_2O)_{3n}$ (**4**), have been assembled from four asymmetric semirigid multicarboxylate ligands 3-(4-carboxy-phenoxy)-phthalic acid (H_3L^1), 3-(2-carboxy-phenoxy)-phthalic acid (H_3L^2), 4-(2-carboxy-phenoxy)-phthalic acid (H_3L^3), and 4-(4-carboxy-phenoxy)-phthalic acid (H_3L^4) with the help of 4,4′-bipyridine (4,4′-bpy) ligand. X-ray single crystal diffraction analysis reveals that compound **1** displays a one-dimensional (1D) zigzag chain structure constructed from 4,4′-bpy ligands and partly deprotonated L^1 ligands, which further forms a three-dimensional (3D) supramolecular architecture via hydrogen bonds. Complex **2** possesses a two-dimensional (2D) layered architecture composed of continuous trinuclear Co(II) clusters. Complex **3** also shows a 2D molecular framework assembled from alternate tetranuclear and dinuclear Co(II) clusters bridged by 4,4′-bpy or L^3 ligands, and complex **4** exhibits a 3D (4,4)-connected self-penetrating network constructed from ladder-like and fishbone-like subunits. Magnetic studies indicate the spin−orbit coupling of isolated Co(II) in **1** and the overall antiferromagnetic interaction in **2**−**4**.

Introduction

In the field of supramolecular chemistry and crystal engineering, the design and assembly of metal−organic coordination frameworks (MOFs) with appealing structures and properties have stimulated interests of chemists in recent years.[1,2] Thus far, a large number of metal−organic coordination polymers have been prepared.[1−3] The molecular structures of MOFs have been revealed to mainly depend on the coordination geometries and sites of the organic ligands.[4] However, there still remains a great challenge for directional construction of functional MOFs with predictable molecular structures and expected properties because of many subtle factors related with the crystallization process.

In the past few years, multidentate O-donor ligands including 1,4-benzenedicarboxylate and 1,3,5-benzenetribenzoate with a rigid benzene central molecular framework[5] as well as 1,4-cyclohexanedicarboxylate and tetrahydrofurantetercarboxylate with flexible cyclohexane or tetrahydrofuran central molecular framework[6] were extensively employed for the preparation of functional MOFs. Quite recently, a new family of multidentate O-donor ligands with a semirigid V-shaped molecular framework, actually two benzene rings connected by an nonmetallic atom (C, O, S, and N atoms) including 2,2′,3,3′-oxidiphthalic acid, 4,4′-oxidiphthalic acid, 3,3′,4,4′-oxidiphthalic acid, and 4,4′-(hexafluoroisopropyl idene)-bis(benzoic acid), have been used to construct MOFs, leading to interesting molecular structures including helices and interpenetrating networks as well as potential applications in the field of separation, absorption, catalysts, and sensors.[7] As can be seen, the majority of coordination polymers assembled from these semirigid V-shaped multidentate O-donor ligands with carboxylic substituents at symmetrical positions possess discrete metals as node, leading to the limitation in tuning the functionality of MOFs. However, the semirigid V-shaped multidentate O-donor ligands with carboxylic substituents at asymmetrical positions of a V-shaped central molecular framework have been scarcely explored,[8] to the best of our knowledge. For the purpose of constructing MOFs with tunable structures and properties, it seems interesting to develop new semirigid V-shaped multidentate O-donor ligands with carboxylic substituents at asymmetrical positions of a central molecular framework. These ligands are expected to assemble new MOFs with novel structural motifs due to their different coordination modes and molecular conformations.

In the present paper, four multidentate O-donor ligands with three coordinating carboxylic groups attached at asymmetrical positions of a semirigid V-shaped central molecular framework, namely, 3-(4-carboxy-phenoxy)-phthalic acid (H_3L^1), 3-(2-carboxy-phenoxy)-phthalic acid (H_3L^2), 4-(2-carboxy-phenoxy)-phthalic acid (H_3L^3), and 4-(4-carboxy-phenoxy)-phthalic acid (H_3L^4), were synthesized. Using these four semirigid V-shaped multicarboxylate ligands with the help of a 4,4′-bpy secondary ligand, a series of four novel Co(II) MOFs with diverse molecular structures including $[Co(HL^1)(\mu\text{-}4,4'\text{-bpy})(H_2O)_3]_n\cdot(4,4'\text{-bpy})_n\cdot(H_2O)_{2n}$ (**1**), $[Co_{1.5}(L^2)(\mu\text{-}4,4'\text{-bpy})_{1.5}]_n\cdot(4,4'\text{-bpy})_{0.5n}$ (**2**), $[Co_3(L^3)(HL^3)(OH)(H_2O)_2(\mu\text{-}4,4'\text{-bpy})_2]_n\cdot(H_2O)_{2.5n}$ (**3**), and $[Co_{1.5}(L^4)(\mu\text{-}4,4'\text{-bpy})_2(H_2O)_3]_n\cdot(H_2O)_{3n}$ (**4**) were prepared. Their single crystal structures and magnetic properties have been systematically investigated.

It is worth noting that the coordination polymers constructed directly from these four asymmetric semirigid V-shaped multidentate O-donor ligands L^1−L^4 have not been reported thus far. The sole silver complex of L^4 ligand was obtained by case from the reaction between symmetric 3,3′,4,4′-oxidiphthalic acid and silver salt during a hydrothermal process.[9]

Experimental Section

All reagents and solvents employed in the present work were obtained from the commercial source and used directly without

*To whom correspondence should be addressed. E-mail: jzjiang@sdu.edu.cn.

further purification. These four ligands were synthesized according to the reported procedure as detailed below.[10]

Synthesis of Semirigid Asymmetric Ligands H_3L^1−H_3L^4. The ligand of 3-(4-carboxy-phenoxy)-phthalic acid (H_3L^1) was synthesized according to the following procedure. To a solution of methyl-4-hydroxybenzoate (3.04 g, 0.02 mol) and anhydrous Na_2CO_3 (2.12 g, 0.02 mol) in DMF (25 mL) stirred for 30 min, 3-nitropthalonitrile (3.46 g, 0.02 mol) was added. The resulting mixture was stirred for 24 h. Then the mixture was poured into water (200 mL), and a slightly yellow solid was yielded and isolated by filtration. The crude product was dried in air, yielding methyl-4-(3,4- dicyanophenoxy)benzoate (4.45 g, 80%).

The mixture of 4-(2,3-dicyano-phenoxy)-benzoic acid methyl ester (2.78 g, 0.01 mol) and NaOH (2.40 g, 0.06 mol) in distilled water (150 mL) was refluxed until the solution turned clear. The solution was then cooled down to room temperature and filtered. After the pH value of the filtrate was adjusted to about 5−6 with HCl (6.0 mol/L), the filtrate was kept undisturbed at room temperature. After about one day, a large amount of white solid of H_3L^1 was collected by filtration with a yield of 2.20 g, 73%. IR/cm^{-1} (KBr): 3405 (m), 3066 (m), 1702 (s), 1580 (m), 1419 (m), 1253 (s), 1159 (s), 961 (m), 801 (m), 755 (m). ^{1}H NMR (300 MHz, DMSO-d_6): δ 7.169 (d, J = 8.7 Hz, 1H), δ 7.303 (d, J = 0.8.1 Hz, 1H), δ 7.667 (t, J = 8.1 Hz, 1H), δ 7.891 (d, J = 7.8 Hz, 1H), δ 7.982 (d, J = 0.8.7 Hz, 1H), 11.344 (s, 3H).

By employing the above-described procedure used to prepare H_3L^1 with corresponding nitropthalonitrile and hydroxybenzoate methyl ester as the starting materials, the other three ligands H_3L^2, H_3L^3, and H_3L^4 have been prepared with the yield of 2.78 g (89%), 2.47 g (82%), and 2.63 g (87%), respectively. For H_3L^2, IR/cm^{-1} (KBr): 3440 (m), 2903 (m), 1694 (s), 1598 (m), 1455 (m), 1283 (s), 1091 (s), 844 (m), 754 (m). ^{1}H NMR (300 MHz, DMSO-d_6): δ 6.947 (d, J=8.1 Hz, 1H), δ 6.020 (d, J=0.8.4 Hz, 1H), δ 7.296 (t, J=7.8 Hz, 1H), δ 7.486 (t, J=7.8 Hz, 1H), δ 7.556 (t, J=0.7.8 Hz, 1H), δ 7.671 (d, J=7.8 Hz, 1H), δ 7.842 (d, J=0.7.8 Hz, 1H), δ 11.335 (s, 3H). For H_3L^3, IR/cm^{-1} (KBr): 3382 (m), 3069 (m), 1697 (s), 1605 (m), 1413 (m), 1233 (s), 1087 (s), 852 (m), 801 (m), 757 (m). 1H NMR (300 MHz, DMSO-d_6): δ 6.959 (d, J=8.7 Hz, 1H), δ 7.065 (d, J= 0.7.8 Hz, 1H), δ 7.289 (t, J=8.1 Hz, 1H), δ 7.529 (t, J=8.4 Hz, 1H), δ 7.709 (s, 1H), δ 7.931 (d, J=7.8 Hz, 1H), δ 7.977 (d, J=0.7.8 Hz, 1H), δ 11.275 (s, 3H). For H_3L^4, IR/cm^{-1} (KBr): 3431 (m), 3080 (m), 1677 (s), 1597 (s), 1427 (m), 1265 (s), 1236 (s), 814 (m), 749 (m). ^{1}H NMR (300 MHz, DMSO-d_6): δ 7.166 (d, J=9.0 Hz, 1H), δ 7.263 (d, J=0.8.7 Hz, 1H), δ 7.764 (s, 1H), δ 8.011 (d, J=0.9.0 Hz, 1H), δ 8.274 (d, J=0.8.7 Hz, 1H), 11.381 (s, 3H).

General Synthesis Procedure for Complexes 1−4. The target complexes were obtained by utilizing the hydrothermal method with the same stoichiometric ratio for the starting materials in the absence of any base. A Teflon-lined stainless steel container (25 mL) was employed as a reaction vessel containing all starting materials, which was heated to an appropriate temperature and held for 72 h, then cooled to 50 °C at a descent rate of 10 °C/h. Finally, the oven was cut off and kept for another 10 h, and perfect crystals were isolated with a high yield based on the ligand.

$[Co(HL^1)(\mu$-4,4′-bpy$)(H_2O)_3]_n\cdot(4,4'$-bpy$)_n\cdot(H_2O)_{2n}$ (1). A mixture containing $Co(OAc)_2\cdot 4H_2O$ (0.0498 g, 0.2 mmol), 4,4′-bpy (0.0312 g, 0.2 mmol), H_3L^1 (0.0302 g, 0.1 mmol), and H_2O (15 mL) was sealed in a Teflon-lined stainless steel reactor and heated to 120 °C. Slightly purple block-shaped crystals were separated by filtration and dried in air. Yield 0.0319 g, 42% (based on ligand). Anal. Calcd. for $C_{35}H_{34}CoN_4O_{12}$: C 55.20, H 4.50, N 7.36. Found: C 55.48, H 4.50, N 7.35. IR /cm^{-1} (KBr): 3508 (m), 3372 (m), 3068 (m), 1604 (s), 1556 (s), 1462 (m), 1391 (s), 1245 (s), 1063 (m), 819 (m), 781 (m).

$[Co_{1.5}(L^2)(\mu$-4,4′-bpy$)_{1.5}]_n\cdot(4,4'$-bpy$)_{0.5n}$ (2). By employing the above-described procedure with H_3L^2 (0.0302 g, 0.1 mmol) instead of H_3L^1 (0.0302 g, 0.1 mmol) as the starting material, purple blocked crystals were obtained after the reactor was cooled to room temperature from 120 °C with a yield of 0.0574 g, 41% (based on ligand). Anal. Calcd. for $C_{35}H_{23}Co_{1.5}N_4O_7$: C 60.06, H 3.31, N 8.00. Found: C 60.98, H 3.30, N 7.92. IR /cm^{-1} (KBr): 3061 (m), 1606 (s), 1578 (s), 1414 (m), 1383 (s), 1217 (m), 1069 (m), 817 (m), 747 (m).

$[Co_3(L^3)(HL^3)(OH)(H_2O)_2(\mu$-4,4′-bpy$)_2]_n\cdot(H_2O)_{2.5n}$ (3). A mixture of $Co(OAc)_2\cdot 4H_2O$ (0.0498 g, 0.2 mmol), 4,4′-bpy (0.0312 g, 0.2 mmol), H_3L^3 (0.0302 g, 0.1 mmol), and H_2O (15 mL) was sealed in a 25 mL Teflon-lined stainless steel reactor and heated to 150 °C. Violet block-shaped crystals suitable for X-ray diffraction analysis were separated by filtration with a yield of 0.0407 g, 34% (based on ligand). Anal. Calcd. for $C_{50}H_{42}Co_3N_4O_{20}$: C, 50.23, H 3.54, N 4.69. Found: C 50.01, H 3.52, N 4.59. IR /cm^{-1} (KBr): 3616 (m), 3428 (m), 3065 (m), 1607 (s), 1560 (s), 1419 (s), 1270 (m), 1226 (s), 1222 (s), 809 (m), 732 (m).

$[Co_{1.5}(L^4)(\mu$-4,4′-bpy$)_2(H_2O)_3]_n\cdot(H_2O)_{3n}$ (4). A mixture of $Co(OAc)_2\cdot 4H_2O$ (0.0498 g, 0.2 mmol), 4,4′-bpy (0.0312 g, 0.2 mmol), H_3L^4 (0.0302 g, 0.1 mmol), and H_2O (15 mL) was sealed in 25 mL Teflon-lined stainless steel reactor and heated to 120 °C. Purple block-shaped crystals suitable for X-ray diffraction analysis were separated by filtration with the yield of 0.0461 g, 57% (based on ligand). Anal. Calcd. for $C_{35}H_{35}Co_{1.5}N_4O_{13}$: C 52.02, H 4.37, N 6.93. Found: C 52.01, H 4.32, N 6.89. IR /cm^{-1} (KBr): 3377 (m), 3038 (m), 1610 (s), 1551 (s) 1410 (s), 1379 (s), 1251 (s), 1222 (s), 1155 (m), 1069 (m), 807 (m), 780 (m).

Physical Measurements. Elemental analyses were carried out with an Elementary Vario El. The infrared spectroscopy on KBr pellets was performed on a Magna-IR 750 spectrophotometer in the region of 4000−400 cm^{-1}. Variable-temperature magnetic susceptibility measurements were performed on a Quantum Design MPMS SQUID magnetometer. The experimental susceptibilities were corrected for the diamagnetism of the constituent atoms (Pascal's tables). Thermogravimetric analysis (TGA) was performed on a Perkin-Elmer TG-7 analyzer heated from 30 to 600 °C under nitrogen.

Single Crystal X-ray Diffraction Determination. Crystal data for all the four complexes were collected on a Bruker SMART APEXII CCD diffractometer with graphite monochromatic Mo Kα radiation (λ = 0.71073 Å) using the SMART and SAINT programs at 298 K. The structures were solved by the direct method (SHELXS-97) and refined by full-matrix least-squares (SHELXL-97) on F^2. Anisotropic thermal parameters were used for the non-hydrogen atoms and isotropic parameters for the hydrogen atoms. Hydrogen atoms were added geometrically and refined using a riding model. The "isor" order has been used in the refinement of **3**. Crystallographic data and other pertinent information for all the complexes are summarized in Table 1. Selected bond distances and bond angles with the estimated standard deviations are listed in Table S1 (Supporting Information). CCDC 734795−734797 for complexes **1**−**3** and CCDC 709623 for **4** contain the supplementary crystallographic data for this paper. These data can be obtained free of charge from the Cambridge Crystallographic Data Centre via www.ccdc.cam.ac.uk/data_request/cif.

Table 1. Crystal Data and Structure Refinements of Complexes 1−4

compound	1	2	3	4
formula	$C_{35}H_{34}CoN_4O_{12}$	$C_{35}H_{23}Co_{1.5}N_4O_7$	$C_{50}H_{42}Co_3N_4O_{20}$	$C_{35}H_{35}Co_{1.5}N_4O_{13}$
fw	761.59	699.97	1195.67	808.07
crystal system	triclinic	triclinic	triclinic	triclinic
space group	$P\bar{1}$	$P\bar{1}$	$P\bar{1}$	$P\bar{1}$
a	10.7673(10)	11.4757(11)	10.7510(6)	9.3521(9)
b	11.7146(11)	1.5865(12)	12.8281(7)	11.3471(12)
c	14.4532(13)	11.9419(12)	19.6230(14)	18.8078(18)
α	110.2710(10)	86.534(2)	105.9970(10)	79.460(2)
β	94.099(2)	76.535(2)	94.8720(10)	79.462(2)
γ	94.9960(10)	69.576(2)	107.6900(10)	66.512(2)
V	1693.5(3)	1446.7(3)	2436.1(3)	1786.2(3)
Z	2	2	2	2
ρ_{calcd} (g /cm^3)	1.494	1.607	1.630	1.502
μ mm^{-1}	0.579	0.931	1.097	0.777
F(000)	790	715	1222	835
R_1 ($I > 2\theta$)	0.0324	0.0365	0.0391	0.0487
R_{w2} ($I > 2\theta$)	0.0954	0.1001	0.1137	0.1117
R_{w2} for all	0.1000	0.1173	0.1180	0.1234
GOF on F^2	1.080	1.093	1.062	0.997

Results and Discussion

Synthesis of the Tricarboxylate Ligands and Complexes 1−4. As shown in Scheme 1, four precursors of the tricarboxylate ligands are synthesized easily by a nucleophilic

Scheme 1. Schematic Molecular Structure of H_3L^1−H_3L^4

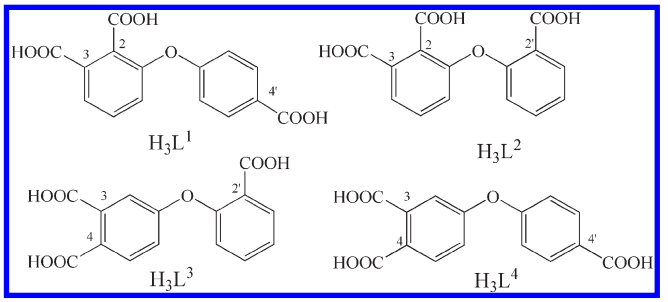

replacing reaction of the corresponding nitropthalonitrile and 4-hydroxybenzoate methyl or 2-hydroxybenzoate methyl in the presence of anhydrous Na_2CO_3 in DMF solution. The resulting precursors are transformed into corresponding multicarboxylate ligands through a hydrolyzation reaction of cyanide and ester groups. These four target asymmetric semirigid V-shaped multicarboxylate ligands 3-(4-carboxy-phenoxy)-phthalic acid (H_3L^1), 3-(2-carboxy-phenoxy)-phthalic acid (H_3L^2), 4-(2-carboxy-phenoxy)-phthalic acid (H_3L^3), and 4-(4-carboxy-phenoxy)-phthalic acid (H_3L^4) are isolated by filtration and used in a hydrothermal reaction without further purification.

In the present study, complexes **1**−**4** were prepared from the hydrothermal reaction between corresponding ligands and Co(OAc)$_2$·4H$_2$O together with 4,4′-bpy secondary ligand in a molar ratio of 1:2:2. A series of reactions were performed to investigate the effect of pH value and reaction temperature on the supramolecular structure of MOFs formed from these four asymmetric H_3L^1−H_3L^4 ligands. The reactions between corresponding tricarboxylate ligands and Co(OAc)$_2$·4H$_2$O salt without 4,4′-bpy as a secondary ligand were performed at a different temperature, giving only some precipitates. However, when the suitable auxiliary N-donor ligand 4,4′-bpy was introduced, perfect single crystals of four complexes were obtained. In addition, when solid NaOH was used to deprotonate these four ligands completely with a molar ratio 3:1 to the tricarboxylate ligand in the absence or presence of 4,4′-bpy ligands, only complex **4** was isolated, indicating the important role of pH value on the formation of MOFs. Similar to the important effect of pH value, reaction temperature also plays an important role in the preparation of these complexes, and complex **3** can be obtained only at a higher temperature.

IR Spectra. In the IR spectra of asymmetric semirigid V-shaped ligands, the absorption band at 1702, 1694, 1697, and 1670 cm^{-1} for the H_3L^1−H_3L^4 ligand, respectively, is attributed to the asymmetric stretching vibration of uncoordinated carboxylic groups, which red-shifts to the range of 1604−1610 cm^{-1} in the spectra of complexes **1**−**4** due to the formation of the Co(II)−O coordination bond of carboxylic oxygen atom in these two ligands.

Crystal Structure of Complex 1. The molecular structure of compound **1** is shown in Figure 1. The asymmetric unit contains one Co(II) ion, one HL^1 ligand, two half coordinated 4,4′-bpy ligands, two half uncoordinated 4,4′-bpy ligands, two coordinated water molecules, and two solvent water molecules. The Co(II) ion is six-coordinated by two nitrogen atoms of 4,4′-bpy ligands, one oxygen atom of HL^1 ligand, and three oxygen atoms from coordinated water molecules, resulting in a distorted octahedral coordination geometry. The neighboring Co(II) ions are linked by 4,4′-bpy ligands with the average distance of 11.73 Å, generating

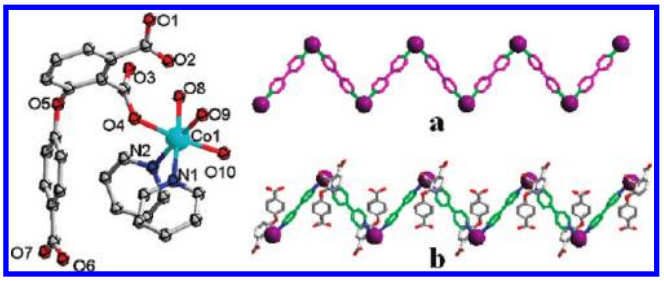

Figure 1. ORTEP drawing of complex **1** (left) and its 1D zigzag chain (right a and b).

Table 2. Selected Hydrogen-bonding Geometry for 1 (in Å and deg)[a]

D−H···A	d(D···H)	d(H···A)	d(D···A)	∠DHA
O7−H7A···N3#1	1.175	1.395	2.550	165.90
O8−H8A···N4#2	0.856	1.954	2.806	173.63
O8−H8B···O3	0.865	1.788	2.625	162.12
O9−H9A···O2#3	0.942	1.712	2.649	173.48
O9−H9B···O2	0.805	2.004	2.781	162.07
O10−H10A···O1#4	0.834	1.825	2.659	177.82
O10−H10B···O11	0.868	1.919	2.787	177.21
O11−H11A···O12#5	0.853	1.976	2.810	165.86
O11−H11B···O6#6	0.855	2.013	2.847	164.84
O12−H12A···O3	0.854	2.175	2.805	130.44

[a] Symmetry codes: #1 $x-1, y, z$; #2 $-x+2, -y, -z$; #3 $-x+2, -y, -z$; #4 $-x+2, -y, -z$; #5 $x-1, y, z$; #6 $x, y+1, z$.

an infinitely 1D zigzag chain, Figure 1. The partly deprotonated L^1 ligand coordinates to Co(II) ion in simple monodentate fashion, Figure S1 (Supporting Information), and the dihedral angle of two aromatic rings is 81.81°.

It is worth noting that the individual zigzag chains are connected into a 3D intricate network via hydrogen bonding interactions. There are abundant hydrogen-bond donors (water molecules and undeprotoned carboxylic groups) and hydrogen-bond acceptors (4,4′-bpy molecules and deprotonated carboxyl groups) to construct a hydrogen bond network, Table 2. The individual chains generate a 2D wall-like layered structure with small windows formed via the first type of hydrogen bonds O−H···O between the coordinated water molecules. Each window is filled by one uncoordinated 4,4-bpy ligand bound to carboxylic groups via the second type of hydrogen bond O−H···N interaction, Figure S2 (Supporting Information). The structure can be depicted as a honeycomb filled with honeybees. The neighboring wall-like layers are further stacked via the third type of hydrogen bond O−H···N interaction between the uncoordinated 4,4′-bpy and coordinated H_2O molecules, giving a 3D supramolecular structure with pseudocavities (11.73 × 18.86 Å), Figure 2. It is worth noting that a complicated supramolecular architecture like **1** assembled via hydrogen bond interactions from simple chains still remain rare, to the best of our knowledge.

Crystal Structures of Complex 2. X-ray single crystal diffraction analysis reveals that **2** crystallizes in the $P\bar{1}$ space group and exhibits a 2D layered framework. The asymmetric unit consists of one and half Co(II) ions, one L^2 ligand, one and half coordinated 4,4′-bpy ligands, and a half uncoordinated 4,4′-bpy ligand. In two crystallographically independent Co(II) ions, Co1 ion locates in an inverse center and is coordinated by two nitrogen atoms of 4,4′-bpy ligands, and four oxygen atoms from two L^2 ligands; Co2 ion possesses a distorted octahedral coordination geometry with two nitrogen atoms of 4,4′-bpy ligands occupying axis positions and four oxygen atoms of three L^2 ligands forming an equatorial

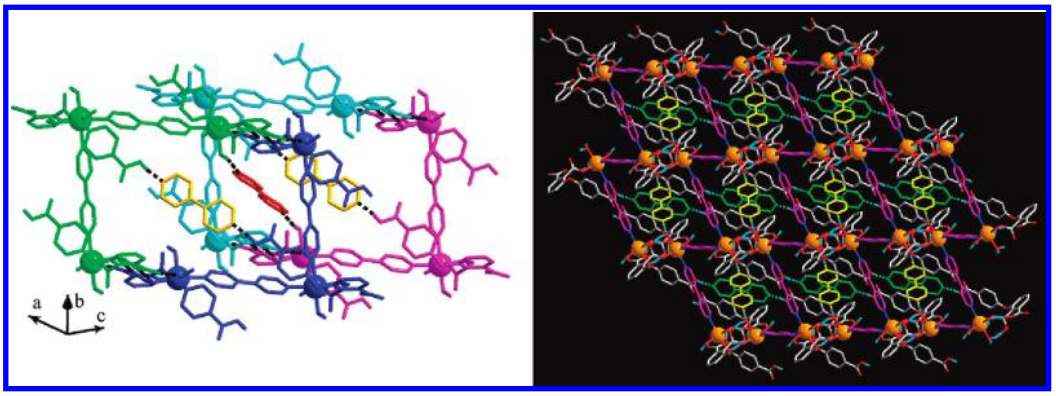

Figure 2. Details of the hydrogen bond connection of 1 (left) and 3D supramolecular structure along the *c* axis (right), highlighting the two types of uncoordinated 4,4′-bpy molecules in the cavities.

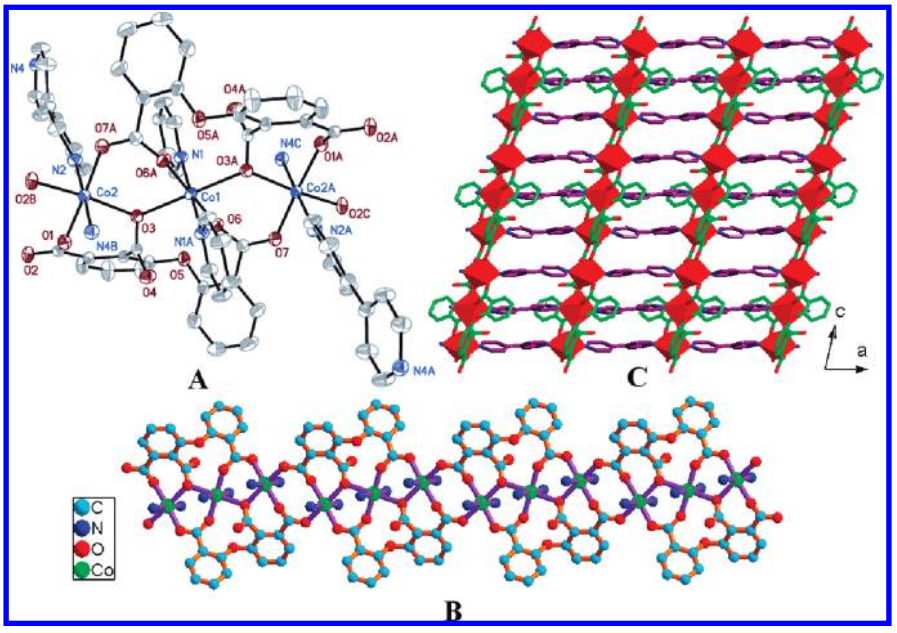

Figure 3. ORTEP drawing about the basic building block, the local connectivity, and the coordination environment for atoms of 2: (A) a trinuclear cluster, (B) a 2D layered network, and (C) a 1D infinite chain composed of continuous trinuclear Co(II) clusters.

plane. Through the inverse center, a linear trinuclear Co(II) cluster is given by two crystallographically equivalent Co2 and Co2A ions in terminal positions and one Co1 ion in the center, Figure 3A. The Co1 and Co2 ions are separated by an oxygen atom of carboxylic group as well as an O−C−O bridge of one carboxylic group in a syn−anti coordination mode with a distance of 3.838(6) Å, Figure S1 (Supporting Information). The angle of Co1−O−Co2 is 118.17(8)°. The repeatedly trinuclear subunits are linked by two carboxylic groups in a syn−anti coordination mode coordinating to neighboring terminal Co(II) ions, leading to a 1D infinite chain. The two neighboring terminal Co(II) ions in different trinuclear secondary building units are separated with a distance of 7.675(3) Å. In the chain, the string of the metal ions is surrounded by the two lateral organic ligands in cis-coordination conformation, Scheme 2 and Figure 3B. These 1D chains are connected by 4,4′-bpy ligands, further generating to a 2D layered network, Figures 3C and S3 (Supporting Information). The average length of adjacent Co(II) ions bridged by 4,4′-bpy ligands is 11.47(7) Å. In addition, there are uncoordinated 4,4′-bpy ligands reserved in the cavities formed by the two neighboring layers, Figure S4 (Supporting Information).

Scheme 2. Synthetic Route to Asymmetric Multicarboxylate Ligands H_3L^1−H_3L^4

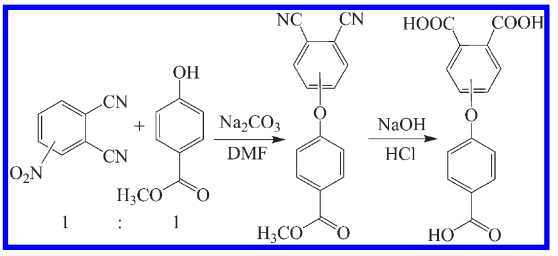

Crystal Structure of Complex 3. The molecular structure of compound **3** is shown in Figure 4. This compound belongs to the $P\bar{1}$ space group and features a 2D network composed of alternate tetranuclear $[Co_4(OH)_2(H_2O)]^{6-}$ and dinuclear Co(II) clusters, Figure 4A,B. The asymmetric unit of **3** contains three crystallographically independent Co(II) ions, two 4,4′-bpy ligands, two L^3 ligands (one containing undeprotonated carboxylic group), one hydroxyl group, two coordinated water molecules, and three guest water molecules. All the three Co(II) ions are located in a distorted octahedral coordination sphere. The coordination geometry of Co1 ion is completed by two

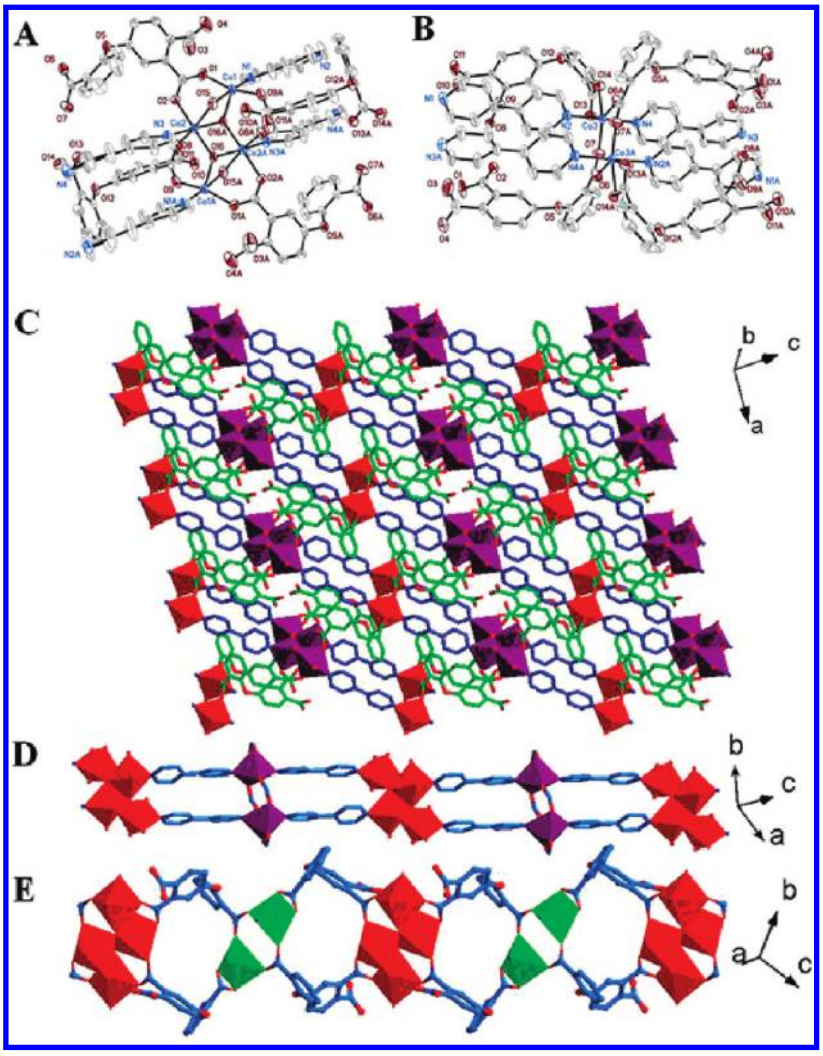

Figure 4. ORTEP drawing about the basic building block, local connectivity, and coordination environment for atoms of **3**: (A) tetranuclear cluster, (B) binuclear cluster, (C) a 2D layered network with teranuclear and dinuclear clusters arranged alternate, (D) ladder-like chain of 4,4′-bpy ligands and Co ions, (E) a ribbon chain of L^3 ligands and Co ions.

oxygen atoms of different carboxylic groups in syn−syn coordination mode from two L^3 ligands, three oxygen atoms from one coordinated water molecule, one μ_2-water molecule, one μ_3-hydrogen group, and one nitrogen atom of 4,4′-bpy ligand. For Co2 ion, the coordination geometry is constructed by one nitrogen atom of 4,4′-bpy ligand and five oxygen atoms from two μ_3-bridged hydroxyl groups, one μ_2-water molecule, and two carboxylic groups in syn−syn coordination mode from different L^3 ligands. For Co3 ion, the coordination environment is formed by two nitrogen atoms from two 4,4′-bpy ligands occupying the axis sites and four oxygen atoms (two from a bidentate chaleting carboxylic group of L^3 ligand and the other two from two carboxylic groups in syn-syn coordination mode form different L^3 ligands) forming the equatorial plane. The distances of Co−O and Co−N bonds span the range of 1.990(2)−2.280(2) and 2.094(2)−2.178(3) Å, which are comparable to those reported for compounds containing O−Co−N segments.[11]

As can be seen in Figure 4C, the tetranuclear Co(II) cluster is surrounded by four dinuclear Co(II) clusters. This is also true for the dinuclear Co(II) cluster. The two Co1 and Co2 ions are connected by two μ_3-bridging hydroxyl groups and two μ_2-linking water molecules to form a centrosymmetric ladder-like tetranuclear subunit, which does not sit in a plane, Figure 4A. In the tetranuclear cluster, the distance of Co1−Co2, Co1−Co2A, and Co2−Co2A is 3.209(2), 3.532(2), and 3.090 Å, respectively, and the angle of Co1−O15−Co2, Co1−O16−Co2A, Co1−O15−Co2A, and Co2−O16−Co2A 119.88(8), 103.92(9), 86.44(10), and 96.80(9)°. Two neighboring crystallographically uniform Co3 ions are linked by two carboxylic groups of different L^3 ligands in syn−syn coordination mode, leading to a dinuclear oligomer with a distance of Co3−Co3A amounting to 4.021(3) Å, Figure 4B. The adjacent tetranuclear and dinuclear clusters are bridged by two 4,4′-bpy ligands, generating an infinite ladder-like motif with 4,4′-bpy ligands as two rails and tetranuclear and dinuclear Co(II) oligomers alternatively playing the role of rungs, Figure 4D. Apart from the 4,4′-bpy bridges, tetranuclear and binuclear clusters are also connected by the two L^3 ligands along the diagonal direction of ladder-type motif in a trans-coordination conformation, generating an infinite 1D ribbon chain, Scheme 2 and Figure 4E. The ladder-like and ribbon chains compile a 2D layered network, Figure 4C. It is worth noting that there are a few complexes containing two kinds of oligo-nuclear Co(II) subunits.[12]

Crystal Structures of Complexes 4. X-ray single crystal diffraction analyses reveal that complex **4** crystallizes in the

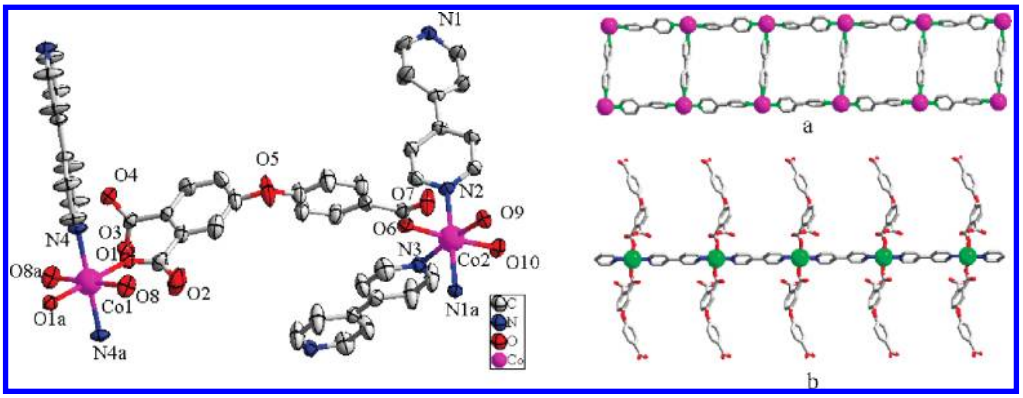

Figure 5. ORTEP drawing about the local coordination environment and connectivity for atoms in the asymmetric unit of **4** (left) and the basic building block (right): (a) ladder-like substructure assembled by 4,4′-bpy ligands and Co(II) ions and (b) the fishbone-like motif formed by 4,4′-bpy, Co(II)ions, and L^4 ligands.

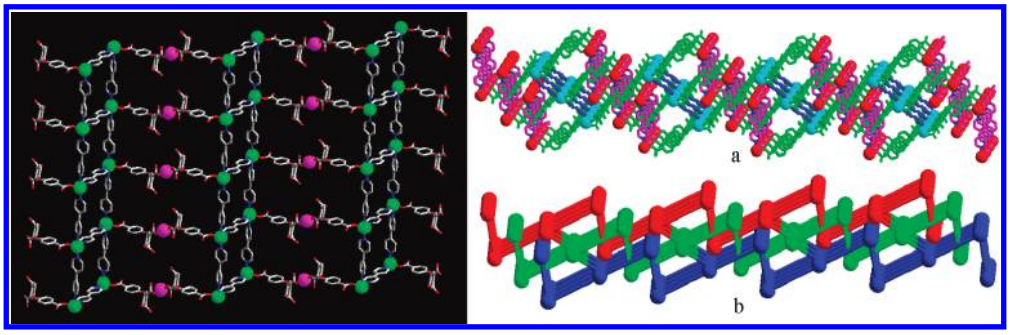

Figure 6. An undulated layer in complex **4** constructed by a ladder-like motif and bridging $[Co(L^4)_2]^{4-}$ moieties without considering 4,4′-bpy connecting Co1 (left) and a self-penetrating network formed (right a and b for structural and topology diagram, respectively).

space group of $P\bar{1}$ and features a (4,4)-connected 3D self-penetrating network. As shown in Figure 5, the asymmetric unit of **4** contains one and half crystallographically independent Co(II) ions, one whole and two-half 4,4′-bpy ligands, one L^4 ligand, three coordinated water molecules, and three guest water molecules. Co1 ion locates in a slightly distorted octahedral coordination sphere with the equatorial plane formed by two oxygen atoms from L^4 ligand and two oxygen atoms of coordinated water, while the axial positions are occupied by two nitrogen atoms from two 4,4′-bpy ligands. Compared to the coordination geometry of the Co1 ion, the Co2 ion has a more strongly distorted octahedral geometry completed by three nitrogen atoms from different 4,4′-bpy ligands, one oxygen atom of L^4 ligand, and two oxygen atoms from coordinated water molecules. The bond length of Co−O and Co−N ranges from 2.125(3) to 2.200(3) Å and 2.076(3) to 2.112(3) Å, respectively, which are comparable to those of reported compounds containing O−Co−N segenments.[11] The dihedral angle of the two aromatic rings connected by the ether oxygen atom is 73.19(3)°.

As shown in Figure 5, the Co2 atom is bridged by 4,4′-bpy ligands as a T-shaped node to form a ladder-like motif, which is found in many other coordination polymers.[13] Interestingly, there is a fishbone-like motif composed of 4,4′-bpy, L^4 ligand, and Co1 atoms, in which the 4,4-bpy ligand coordinates with Co2 atom to form the main skeleton, whereas L^4 ligand plays the role of the side bone. To the best of our knowledge, only several examples containing fishbone-like motif have been reported thus far.[10] In the case that the 4,4′-bpy ligands in the fishbone-like motifs are ignored, the strongly wavy 2D layer structure is assembled by the rails of ladder-like motif connected with a $Co(L^4)_2^{4-}$ linker in an up-to-down mode, which could be depicted in the classical (4,4) network as shown in Figure 6. The extremely undulated layer allows interpenetration by two other layers, one from above and one from below, leading to a 3D pseudo-interpenetrating network, Figure S5 (Supporting Information).[11] Unexpectedly, a self-penetrating network is formed by the undulated layers linked by 4,4′-bpy units. Topology analysis reveals that the complex **4** is a binodal 4-connected self-penetrating network with the vertex symbol $6_2\cdot\infty\cdot8_5\cdot8_5\cdot8_5\cdot8_5$ (node 1) and $4\cdot6\cdot4\cdot6\cdot8_2\cdot\infty$ (node 2), Figure 6.

The Coordination Modes of Tricarboxylate Ligands L^1−L^4. Figure 7 shows different coordination modes of ligands L^1-L^4 exist in complexes **1**−**4**. It is well-known that the organic multicarboxylates as an important O-donor ligand have been widely employed to prepare MOFs not only due to their diverse coordination mode but also their nature to form a supramolecular structure via hydrogen bond interaction. This is also true for the symmetric and asymmetric semirigid V-shaped multicarboxylate ligands. As a consequence, it seems necessary to understand and compare the difference in coordination mode between symmetrical and asymmetrical semirigid V-shaped multicarboxylate ligands for the purpose of directional design and synthesis of functional materials. As can be seen in Figure 7, there are five types of different coordination modes and two kinds of coordination configurations for these four ligands. In compound **1**, L^1 ligand in a trans-typed configuration possesses μ_1-bridging mode with 2-carboxylic group in a

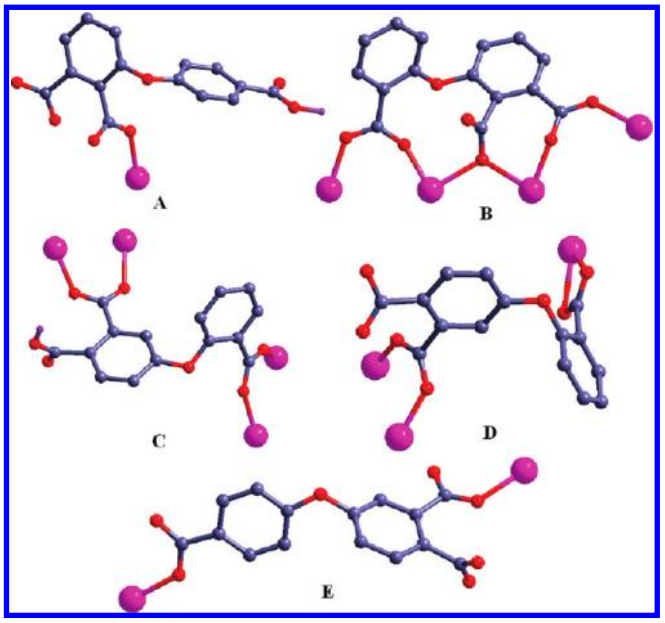

Figure 7. The various coordination modes for L^1-L^4 ligands.

monodentate coordination mode and 4′-carboxylic group undepronated, Scheme 1 and Figure 7A. For **2**, L^2 ligand shows a cis-typed configuration with μ_4-bridging mode, and 2-, 2′-, and 3-carboxylic groups exhibit μ_2-η^2-η^0, μ_2-η^1-η^1, and μ_2-η^1-η^1 coordination mode, respectively. Both the 2′- and 3-carboxylic groups are in syn−anti conformation, Figure S1 (Supporting Information). There are two types of L^3 ligand in **3**, both of which are in μ_4-connected modes, Figure 7C,D. Differently, the 4′-carboxylic groups adopt μ_2-η^1-η^1 didentate mode in syn−syn conformation and μ_2-η^1-η^1 chelating mode, respectively. Similar to the L^3 ligand, the μ_2-bridged L^4 ligand in **4** is in the trans-typed conformation, of which both 3- and 4′-carboxylic groups exhibit μ_1-η^1-η^0 linked mode. As can be found in the present study, the carboxylic groups of $L^1$and L^4 ligands are in the monodentate mode, leading to the discrete metal as node and in turn limiting the propagation of magnetic superexchange between neighboring metal centers effectively. However, the multibridged carboxylic groups of L^2 and L^3 ligands are likely to assemble metal ions into various polymetallic aggregates. In addition, the conformations of these ligands indicate that L^1, L^3, and L^4 in trans-type modes support the formation of 2D or 3D framework of MOFs via covalent or hydrogen bonds. In contrast, L^2 ligand in cis-type configuration only favors the formation of discrete or 1D compound in the absence of any second ligand. The dihedral angle between the three atomic planes of carboxylic group and its benzene ring for the asymmetric ligands L^1-L^4 is consistent with that revealed for symmetric multicarboxylate ligands,[7] Table 3. This is also true for the dihedral angle between the two benzene rings for these four ligands in the range of 68.55−83.52°. At the end of this section, it is worthy noting that complexes with multinuclear clusters as a subunit have been obtained by changing the positions of carboxylic substituents at the V-shaped central molecular framework of these asymmetrical tricarboxylate ligands. Moreover, the effect of asymmetric position for tricarboxylate ligand L^4 is considered to be responsible for the binodal 4-connected molecular structure of **4**.

Table 3. The Dihedral Angles for L^1-L^4 Ligands

	Dihedral angle between of the plane three atomic carboxylic group and its benzene ring (°)		
L^1	2-carboxylic group 24.25	3-carboxylic group 78.36	4′-carboxylic group 7.69
L^2	2-carboxylic group 76.66	3-carboxylic group 2.03	2′-carboxylic group 23.29
L^3	3-carboxylic group 41.08	4-carboxylic group 47.26	2′-carboxylic group 44.66
L^4	3-carboxylic group 18.86	4-carboxylic group 65.86	4′-carboxylic group 22.02

Magnetic Properties of Complexes 1−4. The magnetic properties of **1**−**4** were investigated in the temperature range of 2.0−300.0 K under an outer field of 2000 Oe. As shown in Figure 8, the changing tendencies for temperature dependence of magnetic susceptibility for complexes **1**−**3** are similar. The room temperature value of $\chi_m T$, 3.574 emu K mol^{-1} for **1**, 5.733 emu K mol^{-1} for **2**, 8.240 emu K mol^{-1} for **3**, and 3.063 emu K mol^{-1} for **4**, is bigger than the spin only value of 1.875 emu K mol^{-1} [one isolated Co(II) ions] for **1**, 2.813 emu K mol^{-1} [one and half isolated Co(II) ions] for **2**, 5.625 emu K mol^{-1} [for three isolated spin Co(II) ions] for **3**, and 2.813 emu K mol^{-1} [one and half isolated Co(II) ions] for **4** with $g = 2.00$, respectively. The larger experimental value of these four complexes than corresponding spin only value can be assigned to the unquenched orbital-moment as a result of spin−orbit coupling in the distorted octahedral coordinated Co(II) ions.[14] When the temperature is lowered, the $\chi_m T$ value decreases slowly until about 150 K for **1**−**3** and 30 K for **4**, then decreases quickly to 1.854, 2.230, 0.552, and 2.926 emu K mol^{-1} at 2 K for **1**−**4**, respectively. These results at the high temperature region reveal the antiferromagnetic interaction between neighboring Co(II) ions in these four complexes. In contrast, the decrease of the magnetization at low temperature for Co(II) complexes was due mainly to three factors, namely, intramolecular antiferromagnetic coupling interaction between neighboring Co(II) ions, intermolecular antiferromagnetic coupling interaction, and contribution of the orbital momentum of the single Co(II) ion.[15] The magnetic susceptibilities obey the Curie−Weiss law in the temperature range above 30 K for **1**−**3** and the whole temperature range measured for **4**, giving a negative Weiss constant $\theta = -19.53$ K and Curie constant $C = 3.76$ emu K mol^{-1} for **1**, $\theta = -18.65$ K and Curie constant $C = 6.10$ emu K mol^{-1} for **2**, $\theta = -37.38$ K and $C = 9.36$ emu K mol^{-1} for **3**, as well as $\theta = -0.94$ K and $C = 3.06$ emu K mol^{-1} for **4**, confirming again the antiferromagnetic interaction exhibited in these complexes at the high temperature region. On the basis of the analysis of the crystal structures for complexes **1**−**4**, 4,4′-bpy ligand as the main magnetic exchanging path in complexes **1** and **4** is responsible for the antiferromagnetic interaction accordingly to the related results reported previously.[16] It is worth noting that in contrast to the unremarkable magnetic property of **4**, compound **1** possesses bigger C and θ values, indicating a strong antiferromagnetic interaction between adjacent Co(II) ions linked by 4,4′-bpy ligand in zigzag chain. However, on the basis of the previous result of Co(II) complexes containing long linkers, the negative θ value and deceasing tendency of $\chi_m T$ in the high temperature region should arise from the spin−orbit coupling for the $^4T_{1g}$ state of isolated Co(II) ion possessing an octahedral ligand field.[17] On the basis of an approximate model of isolated Co(II) ion, the magnetic susceptibilities of **1** can be fitted by

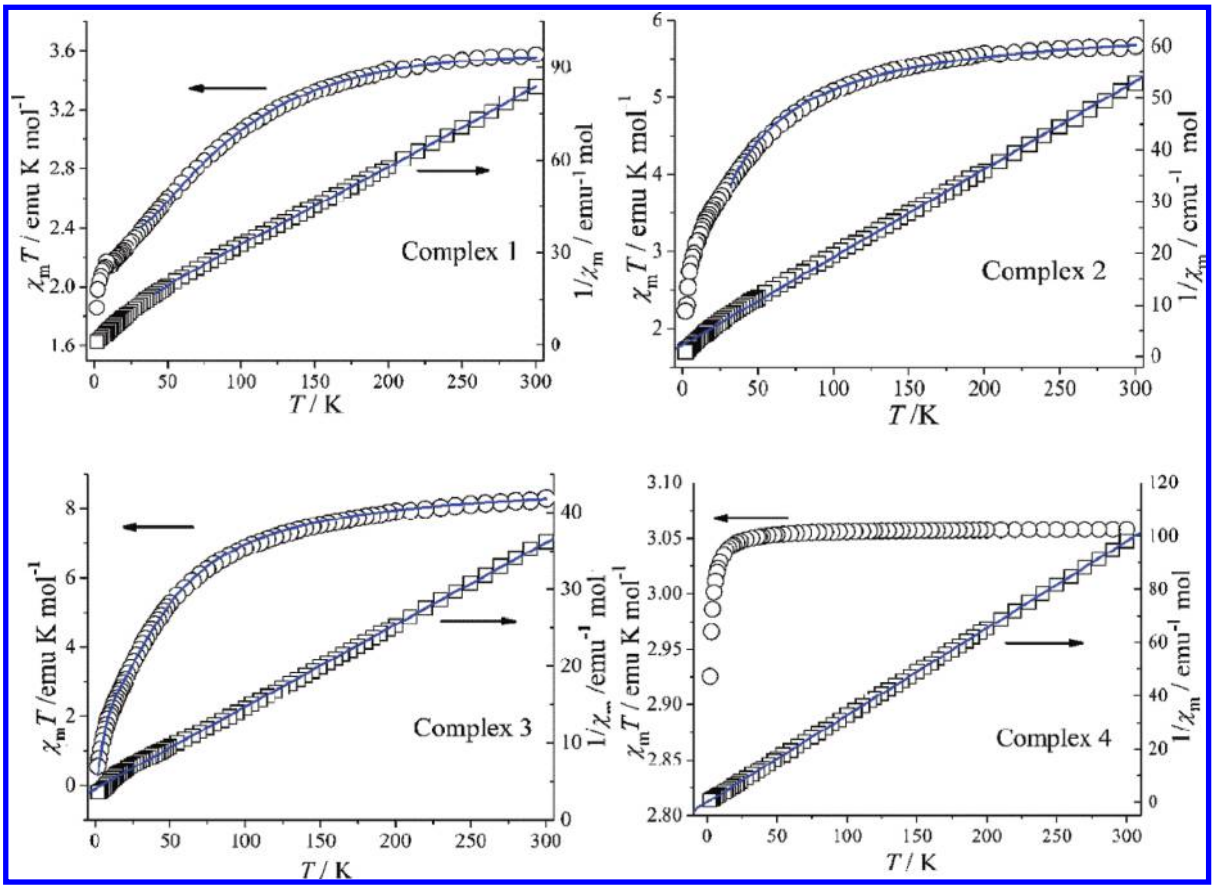

Figure 8. Temperature dependence of $\chi_m T$ for **1**−**4** (the blue solid lines represent the best fitting for complexes **1**−**4**).

the following polynomial expression deduced from $\hat{H} = -\lambda LS$.[18]

$$\chi_{mono} = \frac{1}{T}\left[\frac{7(3-A)^2x}{5} + \frac{12(2+A)^2}{25A} + \left(\frac{2(11-2A)^2x}{45} + \frac{176(2+A)^2}{25A}\right)x\exp\left(\frac{-5Ax}{2}\right) + \left(\frac{(5+A)^2x}{9} - \frac{20(2+A)^2}{27A}\right)\exp(-4Ax)\right] / \left[\frac{8x}{3}\left(3 + 2\exp\left(\frac{-5Ax}{2}\right) + \exp(-4Ax)\right)\right]$$

$$\chi_m = \frac{\chi_{mono}}{1 - (2zJ/Ng^2\beta^2)\chi_{mono}}$$

in which parameter A, λ, and zJ represents a measure of the crystal field strength about the interelection repulsions (1.5 for a weak crystal field, 1.32 for a free ion, and 1.0 for a strong field), spin−orbit coupling parameter (170 cm^{-1} for isolated ions), and total exchange parameter. The best fit of the experimental data for **1** in the range above 30 K gives $\lambda = -116\,\text{cm}^{-1}$, $A = 1.28$, $g = 2.39$, and $zJ = 2.32\,\text{cm}^{-1}$, which are in consistent with the relative values reported previously.[17]

In comparison with the discrete metal ions of **1** and **4** linked by long 4,4′-bpy ligands, the neighboring Co(II) ions of the oligonuclear subunits of **2** and **3** are separated by a shorter distance. This rationalizes the stronger antiferromagnetic interaction for these two complexes. For **2**, it is a layered network containing a 1D metal chain assembled from trinuclear clusters. On the basis of an approximate model of trinuclear Co(II) clusters, the magnetic susceptibility of **2** can be fitted by the following polynomial expression deduced from spin Hamiltonian $\hat{H} = -2J(\hat{S}_1\hat{S}_2 + \hat{S}_2\hat{S}_3)$

$$\chi = Ng^2\beta^2/KT/\times[(165\exp(9J/KT) + 35\exp(-7J/KT) + 8\exp(-12J/KT) + 35\exp(5J/KT) + 99 + 10\exp(-2J/KT) + \exp(-5J/KT) + 84\exp(6J/KT) + 35\exp(-J/KT) + 10\exp(-6J/KT) + \exp(-9J/KT))/(5\exp(9J/KT) + 4 + 3\exp(-7J/KT) + 2\exp(-12J/KT) + 3\exp(5J/KT) + 2\exp(-2J/KT) + 2\exp(-5J/KT) + 4\exp(6J/KT) + 3\exp(-J/KT) + 2\exp(-6J/KT) + \exp(-9J/KT))]$$

$$\chi_m = \frac{\chi}{1 - (2zJ'/Ng^2\beta^2)\chi}$$

The best fit of the experimental data in the range above 30 K gives $J_1 = -6.62\,\text{cm}^{-1}$ $g = 1.98$, and $zJ' = 2.67\,\text{cm}^{-1}$ for **2**, further confirming the antiferromagnetic interaction between the neighboring Co(II) ions in **2**. The coupling constant is consistent with that of similar Co(II) complexes with the neighboring Co(II) ions connected by μ_2-oxygen atom, and the slightly large zJ' value is reasonable since the neighboring trinulcear Co(II) clusters are linked by carboxylic group in syn−anti coordination mode.[19]

Complex **3** consists of alternate tetranuclear and dinuclear Co(II) clusters. In order to evaluate the average strength of coupling between the neighboring Co(II) ions, this complex is treated as two isolated systems composed of tetranuclear and dinuclear clusters, respectively, Figure S6 (Supporting Information). The magnetic susceptibility of **3** can be fitted based on an approximate combination model of tetranuclear and dinuclear Co(II) clusters, and the polynomial expression deduced from spin Hamiltonian $\hat{H} = -2J_1(\hat{S}_1\hat{S}_2 + \hat{S}_2\hat{S}_4 + \hat{S}_2\hat{S}_3 + \hat{S}_3\hat{S}_4 + \hat{S}_4\hat{S}_1) - 2J_2\hat{S}_5\hat{S}_6$ is listed below.

$$\chi = Ng^2\beta^2/KT/ \times [(182\exp(45J_1/2KT) + 220\exp(21J_1/2KT) + 180\exp(J_1/2KT) + 168\exp(-15J_1/2KT) + 30\exp(-27J_1/2KT) + 4\exp(-35J_1/2KT) + 28\exp(-9J_1/2KT) + 2\exp(-11J_1/2KT) + 110\exp(33J_1/2KT) + 120\exp(13J_1/2KT) + 94\exp(-3J_1/2KT) + 6\exp(-23J_1/2KT) + 88\exp(5J_1/2KT) + 48\exp(-7J_1/2KT)/(14\exp(45J_1/2KT) + 22\exp(21J_1/2KT) + 27\exp(J_1/2KT) + 58\exp(-15J_1/2KT) + 15\exp(-27J_1/2KT) + 6\exp(J_1/2KT) + \exp(-39J_1/2KT) + 7\exp(-9J_1/2KT) + 3\exp(-11J_1/2KT) + 11\exp(-33J_1/2KT) + 18\exp(13J_1/2KT) + 19\exp(-3J_1/2KT) + 9\exp(-23J_1/2KT) + 16\exp(5J_1/2KT) + 17\exp(-7J_1/2KT) + \exp(-19J_1/2KT) + (28\exp(9J_1/2KT) + 14\exp(-3J_1/2KT) + 2\exp(-11J_1/2KT))/(7\exp(9J_1/2KT) + 5\exp(-3J_1/2KT) + 3\exp(-11J_1/2KT) + \exp(-15J_1/2KT))]$$

The best fit of the experimental data in the range above 30 K gives $J_1 = -2.44\ cm^{-1}$, $J_2 = -1.41\ cm^{-1}$, and $g = 1.91$ for **3**. These data further confirm the antiferromagnetic interaction between the neighboring Co(II) ions in **3**. The coupling constant is consistent with similar complexes with the neighboring metal ions connected by an oxygen atom and carboxylic group in syn−anti coordination mode, respectively.[8b,20]

Thermal Analysis. The thermal behavior for compounds **1**−**4** was studied to reveal their thermal stability. TGA experiments were performed on pure single crystal samples of complexes **1**−**4** under N_2 atmosphere with a heating rate of 10 °C/min in the range of 30−600 °C.

The thermal curves are exhibited in Figure S7 of the Supporting Information. For complex **1**, the TGA curve shows the water molecules are lost from room temperature to 136 °C, obsd. 11.54%, calcd. 11.87%, and the decomposition temperature of the residual composition spans the range of 169 to 550 °C. For **2**, the curve over weight loss by stage is not observed since this complex does not contain any solvent water molecule. The decomposition temperature of **2** is in the range of 363.9−512.1 °C. The relatively high thermal stability of **2** was also supported by the same powder X-ray diffraction analysis result recorded after heating the sample at 150 and 300 °C, respectively, with that recorded at room temperature, Figure S8 (Supporting Information). For **3**, the weight loss is observed between room temperature to 128.6 °C owing to the release of solvent water molecules (obsd 3.52%, calcd 3.76%). However, it is worth noting that the dehydrated product of **3** after being heated over 150 °C became amorphous powder, which does not exhibit a good PXRD pattern. The decomposition of the organic segment starts at 317.4 °C. For **4**, the weight loss by stage owing to the gradual release of water molecules was observed from room temperature to 182.7 °C with obsd. 12.65%, calcd. 13.38%.

Conclusion

In summary, four asymmetric semirigid V-shaped tricarboxylate ligands have been employed for the first time to construct four Co(II) coordination polymers. Structural investigation of these complexes reveals that the coordination polymers with polymetallic aggregates as node could be obtained by changing the positions of carboxylic groups at the V-shaped central molecular framework of these asymmetrical tricarboxylate ligands. Magnetic studies indicate the spin−orbit coupling of isolated Co(II) in **1** and the overall antiferromagnetic interactions in complexes **2**−**4**. Further systematic work toward fabricating more MOFs with interesting structure and functionalities using asymmetrical ligands is in progress.

Acknowledgment. This work was supported by the National Natural Science Foundation of China and New Teachers Project of Ph.D. Programs Foundation of Ministry of Education of China (No. 200804221007).

Supporting Information Available: X-ray crystallographic files (CIF), diagrams of the structures, selected bond distances and angles and TGA curves of compounds **1**−**4**. This information is available free of charge via the Internet at http://pubs.acs.org/.

References

(1) (a) Yaghi, O. M.; O'Keeffe, M.; Ockwig, N. W.; Chae, H. K.; Eddaoudi, M.; Kim, J. *Nature* **2003**, *423*, 705. (b) Carlucci, L.; Ciani, G.; Proserpio, D. M. *Coord. Chem. Rev.* **2003**, *246*, 247. (c) Leininger, S.; Olenyuk, B.; Stang, P. J *Chem. Rev.* **2000**, *100*, 853. (d) Bradshaw, D.; Claridge, J. B.; Cussen, E. J.; Prior, T. J.; Rosseinsky, M. J. *Acc. Chem. Res.* **2005**, *38*, 273.

(2) (a) Chou, J.-H.; Kosal, M. E.; Nakagaki, S.; Smithenry, D. W.; Wilson, S. R. *Acc. Chem. Res.* **2005**, *38*, 283. (b) Eddaoudi, M.; Moler, D. B.; Li, H.; Chen, B.; Reineke, T. M.; O'Keeffe, M.; Yaghi, O. M. *Acc. Chem. Res.* **2001**, *34*, 319. (c) Hill, R. J.; Long, D. L.; Champness, N. R.; Hubberstey, P.; Schrooder, M. *Acc. Chem. Res.* **2005**, *38*, 337. (d) Férey, G.; Mellot-Draznieks, C.; Serre, C.; Millange, F. *Acc. Chem. Res.* **2005**, *38*, 217.

(3) (a) Batten, S. R.; Robson, R. *Angew. Chem., Int. Ed.* **1998**, *37*, 1460. (b) Batten, S. R. *CrystEngComm* **2001**, *18*, 1. (c) Carlucci, L.; Ciani, G.; Proserpio, D. M. *Coord. Chem. Rev.* **2003**, *246*, 247. (d) Steel, P. J. *Acc. Chem. Res.* **2005**, *38*, 243. (e) Robin, A. Y.; Fromm, K. M. *Coord. Chem. Rev.* **2006**, *250*, 2127. (f) Barnett, S. A.; Champness, N. R. *Coord. Chem. Rev.* **2003**, *246*, 145.

(4) (a) Evans, O. R.; Xiong, R.; Wang, Z.; Wong, G. K.; Lin, W. *Angew. Chem., Int. Ed.* **1999**, *38*, 536. (b) Kitagawa, S.; Kitaura, R.; Noro, S. *Angew. Chem., Int. Ed.* **2004**, *43*, 2334. (c) Hollingsworth, M. D. *Science* **2002**, *295*, 2410. (d) Férey, G. *Chem. Mater.* **2001**, *13*, 3084.

(5) (a) Eddaoudi, M.; Kim, J.; Rosi, N.; Vodak, D.; Wachter, J.; O'Keefe, M.; Yaghi, O. M. *Science* **2002**, *295*, 469. (b) Serre, C.; Millange, F.; Marrot, J.; Férey, G. *Chem. Mater.* **2002**, *14*, 2409. (c) Chun, H.; Jung, H.; Koo, G.; Jeong, H.; Kim, D.-K. *Inorg. Chem.* **2008**, *47*, 5355. (d) Xu, L.; Choi, E.-Y.; Kwon, Y.-U. *Inorg. Chem.* **2007**, *46*, 10670. (e) Ye, J.-W.; Wang, J.; Zhang, J. Y.; Zhang, P.; Wang, Y. *CrystEngComm* **2007**, *9*, 515. (f) Bradshaw, D.; Prior, T. J.; Cussen,

E. J.; Claridge, J. B.; Rosseinsky, M. J. *J. Am. Chem. Soc.* **2004**, *126*, 6106. (g) Lin, Z.; Wragg, D. S.; Warren, J. E.; Morris, R. E. *J. Am. Chem. Soc.* **2007**, *129*, 10334.

(6) (a) Bi, W. H.; Cao, R.; Sun, D. F.; Yuan, D. Q.; Li, X.; Wang, Y. Q.; Li, X. J.; Hong, M. C. *Chem. Commun.* **2004**, 2104. (b) Wang, J.; Zhang, Y. H.; Tong, M. L. *Chem. Commun.* **2006**, 3166. (c) Wang, J.; Zheng, L. L.; Li, C. J.; Zheng, Y. Z.; Tong, M. L. *Cryst. Growth Des.* **2006**, *6*, 357–359. (d) Zhang, L.; Zhang, J.; Li, Z. J.; Qin, Y. Y.; Lin, Q. P.; Yao, Y. G. *Chem.—Eur. J.* **2009**, *15*, 989. (e) Zhao, X.; Zhu, G.; Fang, Q.; Wang, Y.; Sun, F.; Qiu, S. *Cryst. Growth Des.* **2009**, *9*, 737.

(7) (a) Wang, X.-L.; Qin, C.; Wang, E.-B.; Li, Y.-G.; Su, Z.-M.; Xu, L.; Carlucci', L. *Angew. Chem., Int. Ed.* **2005**, *44*, 5824. (b) Mahata, P.; Madras, G.; Natarajan, S. *J. Phys. Chem. B* **2006**, *110*, 13759. (c) Li, S.-L.; Lan, Y.-Q.; Ma, J.-F.; Yang, J.; Wei, G.-H.; Zhang, L.-P.; Su, Z.-M. *Cryst. Growth Des.* **2008**, *8*, 1610. (d) Xiao, D.-R.; Wang, E.-B.; An, H.-Y.; Li, Y.-G.; Su, Z.-M.; Sun, C.-Y. *Chem.—Eur. J.* **2006**, *12*, 6528. (e) Lan, Y.-Q.; Li, S.-L.; Shao, K.-Z.; Wang, X.-L.; Du, D.-Y.; Su, Z.-M.; Wang, D.-J. *Cryst. Growth Des.* **2009**, *9*, 737. (f) Chen, X.-L.; Zhang, B.; Hu, H.-M.; Fu, F.; Wu, X.-L.; Qin, T.; Yang, M.-L.; Xue, G.-L.; Wang, J.-W. *Cryst. Growth Des.* **2008**, *8*, 3706. (g) Chu, Q.; Liu, G.-X.; Huang, Y.-Q.; Wang, X.-F.; Sun, W.-Y. *Dalton Trans.* **2007**, 4302.

(8) (a) Su, Y.; Zang, S.; Li, Y.; Zhu, H.; Meng, Q. *Cryst. Growth Des.* **2007**, *7*, 1277. (b) Li, W.; Jia, H.-P.; Ju, Z.-F.; Zhang, J. *Dalton Trans.* **2008**, 5350.

(9) Wu, Q.-R.; Chen, X.-L.; Hu, H.-M.; Qin, T.; Fu, F.; Zhang, B.; Wu, X.-L.; Yang, M.-L.; Xue, G.-L.; Xu, L.-F. *Inorg. Chem. Commun.* **2008**, *11*, 28.

(10) Maglio, G.; Palumbo, R.; Schioppa, A.; Tesauro, D. *Polymer* **1997**, *38*, 5849.

(11) (a) Yang, L.; Crans, D. C.; Miller, S. M.; Cour, A.; Anderson, O. P.; Kaszynski, P. M.; Godzala, M. E.; Austin, L. D.; Willsky, G. R. *Inorg. Chem.* **2002**, *41*, 4859. (b) Lin, J.-G.; Su, Y.; Tian, Z.-F.; Qiu, L.; Wen, L.-L.; Lu, Z.-D.; Li, Y.-Z.; Meng, Q.-J. *Cryst. Growth Des.* **2007**, *7*, 2526.

(12) Liu, C.-M.; Gao, S.; Zhang, D.-Q.; Zhu, D.-B. *Cryst. Growth Des.* **2007**, *7*, 1312.

(13) (a) Losier, P.; Zaworotko, M. J. *Angew. Chem., Int. Ed.* **1996**, *35*, 2779. (b) Wagner, B. D.; McManus, G. J.; Moulton, B.; Zaworotko, M. J. *Chem. Commun.* **2002**, 2176.

(14) (a) Kurmoo, M. *Chem. Soc. Rev.* **2009**, *38*, 1353. (b) Chen, Z.; Li, Y.; Jiang, C.; Liang, F.; Song, Y. *Dalton Trans.* **2009**, 5290.

(15) Hu, X.-X.; Xu, J.-Q.; Cheng, P.; Chen, X.-Y.; Cui, X.-B.; Song, J.-F.; Yang, G.-D.; Wang, T.-G. *Inorg. Chem.* **2004**, *43*, 2261.

(16) Zheng, L.-M.; Wang, X. Q.; Wang, Y. S.; Jacobson, A. J. *J. Mater. Chem.* **2001**, *11*, 1100.

(17) (a) Zang, S.; Su, Y.; Li, Y.; Zhu, H.; Meng, Q. *Inorg. Chem.* **2006**, *45*, 2972. (b) Konar, S.; Mukherjee, P. S.; Drew, M. G. B.; Ribas, J.; Chaudhuri, N. R. *Inorg. Chem.* **2003**, *42*, 2545. (c) Sun, H.-L.; Wang, Z.-M.; Gao, S. *Inorg. Chem.* **2005**, *44*, 2169. (d) Masciocchi, N.; Galli, S.; Sironi, A.; Barea, E.; Navarro, J. A. R.; Salas, J. M.; Tabares, L. C. *Chem. Mater.* **2003**, *15*, 2153.

(18) Figgis, B. N.; Gerloch, M.; Lewis, J.; Mabbs, F. E.; Webb, G. A. *J. Chem. Soc. A* **1968**, 2086.

(19) Zeng, M.-H.; Wu, M.-C.; Liang, H.; Zhou, Y.-L.; Chen, X.-M.; Ng, S.-W. *Inorg. Chem.* **2007**, *46*, 7241.

(20) (a) Canadillas-Delgado, L.; Fabelo, O.; Pasan, J.; Delgado, F. S.; Lloret, F.; Julve, M.; Ruiz-Perez, C. *Inorg. Chem.* **2007**, *46*, 7458. (b) Pan, Z.; Song, Y.; Jiao, Y.; Fang, Z.; Li, Y.; Zheng, H. *Inorg. Chem.* **2008**, *47*, 5162.